Original scientific paper

An oxygen reduction reaction electrocatalyst tuned for hydrogen peroxide generation based on a pseudo-graphite doped with graphitic nitrogen

Kailash Hamal[1], Dipak Koirala[1], Jeremy May[1], Forrest Dalbec[1], Nolan Nicholas[2] and I. Francis Cheng[1,✉]

[1]Department of Chemistry, University of Idaho, 875 Perimeter Dr, MS 2343, Moscow, ID 83844, USA
[2]Nano Lab, 22 Bedford St. Waltham, MA, 02453, USA

Corresponding author: ✉jfcheng@uidaho.edu; Tel: (208) 885-6387

Abstract

The carbon material, GUITAR (pseudo-graphite from the University of Idaho thermolyzed asphalt reaction) can be doped with nitrogen in two prevalent forms. In a previous study N(py)-GUITAR had a predominance of pyridinic and pyrrolic moieties with no graphitic nitrogen. In this study N(g)-GUITAR contains a 9.7 % N atomic abundance, with that fraction consisting of 72.3 % graphitic, 23.7 % pyridinic, and 0 % pyrrolic nitrogen. The two materials allow for the examination of hypotheses regarding the importance of the three different nitrogen moieties in the oxygen reduction reaction (ORR). In the previous investigation, the lack of graphitic nitrogen of N(py)-GUITAR gave a preferred pathway of 4e$^-$ ORR to H_2O. In this investigation, N(g)-GUITAR gave a 2e$^-$ ORR pathway to H_2O_2. This was elucidated by current efficiency and hydrodynamic voltammetry studies. The high predominance of graphitic nitrogen confirms the hypothesis regarding 2e$^-$ vs. 4e$^-$ ORR pathways with N-doped carbon materials. N(g)-GUITAR was also evaluated for parasitic pathways for H_2O_2 production. At -0.95 V vs. Ag/AgCl the combination of current efficiency for H_2O_2 is 96 % in 0.05 M Na_2SO_4 with a production rate of 4.9 mg cm^{-2} h^{-1}, is the highest reported in the literature. This indicates possibilities for water purification and treatment applications, which require 10 to 250 mg L^{-1}, depending on conditions.

Keywords
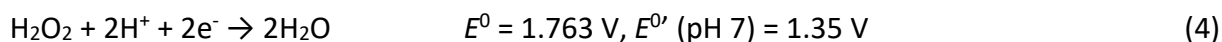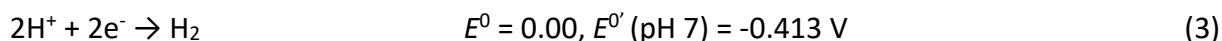Hydrogen peroxide; oxygen reduction reaction; electrocatalysis; N-doped carbon

Introduction

Hydrogen peroxide (H_2O_2) is a relatively eco-friendly and widely used oxidant in the water purification, chemical, and medical industries [1,2]. It is a greener oxidizing agent than chlorine in that it leaves no halogenated by-products such as trihalomethanes and haloacetic acids and is

effective over a wider pH range [3,4]. A partial barrier to wider implementation is that the predominant method of H_2O_2 production, the anthraquinone process, is highly energy-intensive and requires large quantities of extraction solvents [2,3]. Furthermore, transportation issues also hinder its widespread application in water treatment. Onsite generation of H_2O_2 through the electro-chemical process offers minimization of environmental impact as it can be conducted under aqueous and ambient conditions with no hazardous materials or waste [5-7]. This process proceeds by a $2e^-$ electrochemical process outlined in Equation 1.

$$O_2 + 2H^+ + 2e^- \rightarrow H_2O_2 \qquad E^0 = 0.695 \text{ V}, E^{0'} \text{ (pH 7)} = 0.282 \text{ V} \qquad (1)$$

The challenges in the electrochemical production of H_2O_2 are improving slow kinetics and minimizing competing reactions. Slow electrode kinetics gives significant overpotentials for Equation 1 that require electrode potentials from -0.5 to -1.5 V *vs.* Ag/AgCl [8,9]. At these potentials, three other parasitic electrochemical reactions are possible. These include the $4e^-$ oxygen reduction reactions (ORR) to water (Equation 2), the hydrogen evolution reaction (HER), (Equation 3), and the $2e^-$ reduction of H_2O_2 to H_2O (Equation 4) [8-10].

$$O_2 + 4H^+ + 4e^- \rightarrow 2H_2O \qquad E^0 = 1.23 \text{ V}, E^{0'} \text{ (pH 7)} = 0.817 \text{ V} \qquad (2)$$

$$2H^+ + 2e^- \rightarrow H_2 \qquad E^0 = 0.00, E^{0'} \text{ (pH 7)} = -0.413 \text{ V} \qquad (3)$$

$$H_2O_2 + 2H^+ + 2e^- \rightarrow 2H_2O \qquad E^0 = 1.763 \text{ V}, E^{0'} \text{ (pH 7)} = 1.35 \text{ V} \qquad (4)$$

It is therefore incumbent that any electrocatalyst for equation 1 must be selective for this process. This has been noted by several investigators [9,11]. For this contribution, we demonstrate an electrocatalyst that is preferential for the reaction in Equation 1 based on GUITAR (graphite from the University of Idaho thermolyzed asphalt reaction). This carbon material consists of an 85/15 mole ratio of sp^2/sp^3 carbon with a crystallite grain size of 1.5 nm [12,13]. The interlayer d-spacing of 350 pm is slightly expanded over graphite's 335 pm. It is a pseudo-graphite in that it has visual and microscopic features that resemble graphite but has differing properties. Distinguishing characteristics over graphite and other carbon allotropes is that GUITAR has fast heterogeneous electron transfer (HET) kinetics with the $Fe(CN)_6^{4-/3-}$ probe at the basal and edge planes while maintaining excellent corrosion resistance [12-14]. The 3-volt aqueous potential window is among the largest reported. GUITAR is grown using a chemical vapor deposition process, which allows for the fabrication of electrodes ranging from the nano- to macro-sizes, depending on the substrate [12,15,16].

A significant consideration is the tunability of the electrocatalyst for performance and selectively between the reactions of Equations 1-4. Nitrogen doping of carbon materials is associated with the enhancement of electrocatalysis for ORR [17,18]. The C-N bond is believed to facilitate the adsorption of O_2 [19,20]. Predominate forms of N in sp^2 carbon lattices are pyridinic, pyrrolic, N-oxides, and graphitic moieties shown in Figure 1.
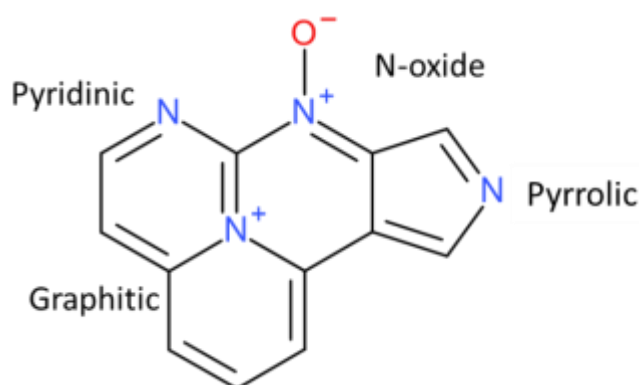

***Figure 1.** Nitrogen moieties in the graphite lattice*

In computational studies, graphitic N is hypothesized to drive the 2e$^-$ process of Equation 1 [21]. However, experimental investigations have only been conducted on mixed nitrogen moiety carbon materials, therefore definitive experimental evidence has yet to be gathered [21-23]. Pyridinic and pyrrolic moieties have been associated with the 4e$^-$ transfer ORR (Equation 2) useful in fuel cell applications [18]. The N-oxide moiety is not associated with any specific ORR pathway. In a previous investigation, a specific nitrogen doping method led to a GUITAR variant with a 0.9 % total nitrogen atomic abundance giving fractions of 0 % graphitic N, 46.0 % pyridinic, 41.3 % pyrrolic, and 12.4 % N-oxide. This electrocatalyst, N(py)-GUITAR, proved to be durable and efficient for the 4e$^-$ transfer ORR to H_2O [15]. An alternative doping method produced a nitrogen-doped pseudo-graphite which contains 9.7 % N [13]. This material, called N(g)-GUITAR, contains graphitic N as the predominant nitrogen moiety [13]. It is noteworthy that GUITAR is the only known carbon material that can be selectively synthesized for predominantly pyridinic/pyrrolic or with graphitic nitrogen moieties. This provides an opportunity to examine the role of these functionalities in the pathway outlined in Equations 1 and 2.

Experimental

Materials and chemicals

KFD graphite felt (SLG Carbon Company, St. Marys, PA, USA) was used as received. The reagents in this investigation were compressed Ar(g) and O_2(g) (>99.5 %, Oxarc, WA, USA), soybean oil (Walmart), paraffin (Gulf Wax), sulfuric acid (96.3 %, J.T Baker Chemical Co, Phillipsburg, NJ, USA). Potassium chloride was obtained from Fisher Scientific (Waltham, NJ, USA), and potassium ferri-cyanide was obtained from Acros Organics (Morris Plains, NJ, USA). Sodium sulfate (EMD Chemicals, Germany), 30 % H_2O_2 (Fisher Scientific, Belgium), and ethanol (99.5 %, Pharmaco, CT, USA) were used without further purification. All aqueous solutions were prepared with deionized water passed through an activated carbon purification cartridge (Barnstead, model D8922, Dubuque, IA).

Electrode fabrication and electrochemical setup

N(g)-GUITAR samples were synthesized using the method described in a previous study [13]. In short, acetonitrile vapors were mixed with N_2 gas and directed into a muffled tube furnace (heated to 900 °C) containing the substrate, for 25 minutes. Quartz wafers, KFD graphite felts, and Ketjen black were used as substrates. Working electrode areas were isolated, as described in the previous study [16]. This was conducted by covering the copper alligator clip to the potentiostat with paraffin wax so as to avoid corrosion of this ohmic contact. Complete wetting of the electrode was conducted by washing with isopropanol followed by deionized water prior to use [24]. All electrochemical studies were conducted in a three-electrode setup cell with Ag/AgCl/3M KCl reference electrode using either a Bioanalytical System CV-50 W (West Lafayette, IN, USA) or a Gamry Instruments Interface 1000 potentiostat. The cell design is shown in Figure 2**.** The cell consisted of anodic and cathodic chambers with a separator membrane composed of cellulose acetate on cellulose paper [25]. This design allows for the formation of H_2O_2 *via* Reaction 1 without consumption at the anode through Reaction 4.

Hydrodynamic experiments were carried out with a Pine Instrument glassy carbon rotating electrode (RDE) (Grove City, PA, USA). For that study, N(g)-GUITAR was deposited on Ketjen black particles and drop-cast onto the RDE disks. This follows a procedure developed in a previous investigation [15].
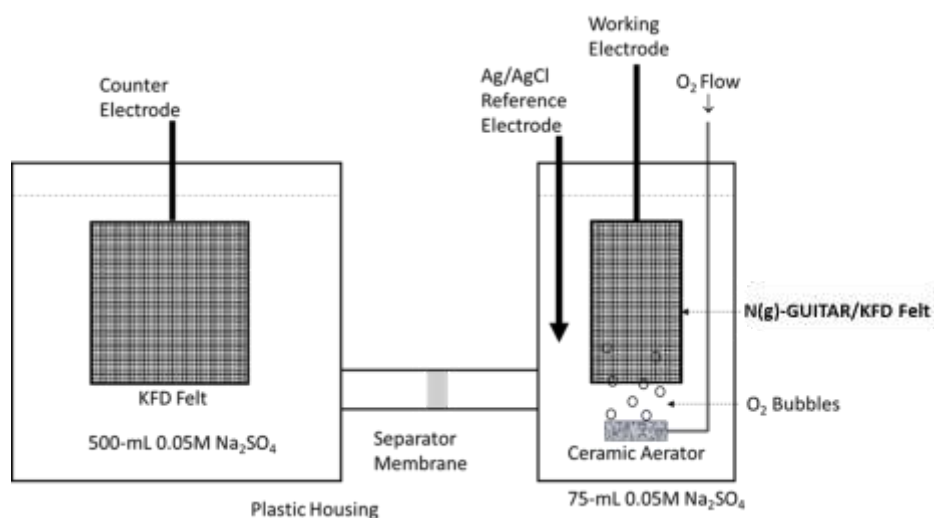
Figure 2. *Electrochemical cell design for H_2O_2 generation*

H_2O_2 analysis

This was conducted by a colorimetric method [26]. Potassium titanium oxide oxalate dihydrate, (Sigma-Aldrich) forms an aqueous complex with H_2O_2, which has an optical absorbance maximum at 400 nm. A Beer's law-based calibration curve was established with H_2O_2 (Pharmaco, CT, USA) standardized with $KMnO_4$ (J.T. Baker Chemical Co, Phillipsburg, NJ, USA) and sodium oxalate (Fisher Scientific, Waltham, NJ, USA).

Results and discussion

Material characterization summary

This material was fully characterized in a previous study [13]. In short, the X-ray photoelectron spectrograph (XPS) of N(g)-GUITAR flakes indicated nitrogen, oxygen, and carbon content of 9.7, 3.9 and 86.4 %, respectively (see Table 1). The deconvolved nitrogen XPS peak revealed 23.7 % pyridinic N (398.2 eV), 60.5 % graphitic N-center (400.98 eV), 11.8 % graphitic N-valley (403.0 eV), and 4 % N-oxides (405.3 eV). This material was notably devoid of pyrrolic nitrogen. Raman spectrographic analysis of N(g)-GUITAR exhibited an I_D/I_G ratio of 1.66, indicating more defects from the inclusion of nitrogen relative to pristine GUITAR (I_D/I_G of 1.15). The XRD analysis of N(g)-GUITAR indicated a similar degree of nano-crystallinity as pristine GUITAR (3.3 nm *vs*. 2.9 nm grain size) [13]. The composition of N(py)-GUITAR is also described in Table 1. Most noticeable is the lack of graphitic N in this electrocatalyst.

Table 1. *Content of total atomic nitrogen and deconvolved nitrogen moiety of N(py)-GUITAR and N(g)-GUITAR, determined via XPS*

	Content of total atomic nitrogen, %	Deconvolved nitrogen moiety, %				
		Graphitic	Pyrrolic	Pyridinic	N-oxides	Reference
N(py)-GUITAR	0.9	0.0	41.3	46.0	12.4	[15]
N(g)-GUITAR (Used in this study)	9.7	72.3	0.0	23.7	4.0	[13]

Formation of the electrocatalyst and surface area

The N(g)-GUITAR electrocatalyst was grown onto a KFD graphite felt substrate using chemical vapor deposition (CVD), as described in a previous study [13]. SEM micrographs of bare KFD fiber and N(g)-GUITAR/KFD are shown in Figure 3. The fiber diameter of KFD (7.4 ± 0.9 μm (n=10)) is within

the range reported in the literature [16,27]. Deposition of N(g)-GUITAR increases this diameter to 10.04 ± 0.9 μm (n = 10). The surface area of 62.2 cm^2 per cm^2 of geometric area for N(g)-GUITAR/KFD was calculated assuming the electrode comprises cylindrical fibers [16,24]. This value agrees with cyclic voltammetric (CV) studies of Fe(CN)$_6^{4-/3-}$ using the Randles-Ševčik equation (Equation 5) below, where i_p, n, A, C (10^{-6} mol cm^{-3}), D (7.26×10^{-6} cm^2 s^{-1}), and v are peak current, number of electrons transferred, area, concentration, diffusion coefficient and potential sweep rate, respectively [16].

$$i_p = 268,600 \, n^{3/2}AC \, (Dv)^{1/2} \tag{5}$$

Figure 4A shows the overlayed CV plots at multiple scan rates. A plot of i_p *vs.* $v^{1/2}$ in Figure 4B indicates semi-infinite linear diffusion with the slope indicating an electrochemically active surface area (ECSA) of 59.0 cm^2 per cm^2 of geometric area. ECSA for GUITAR/KFD and bare KFD are 50.6 and 61.5 cm^2 per cm^2 of geometric area, respectively [16].
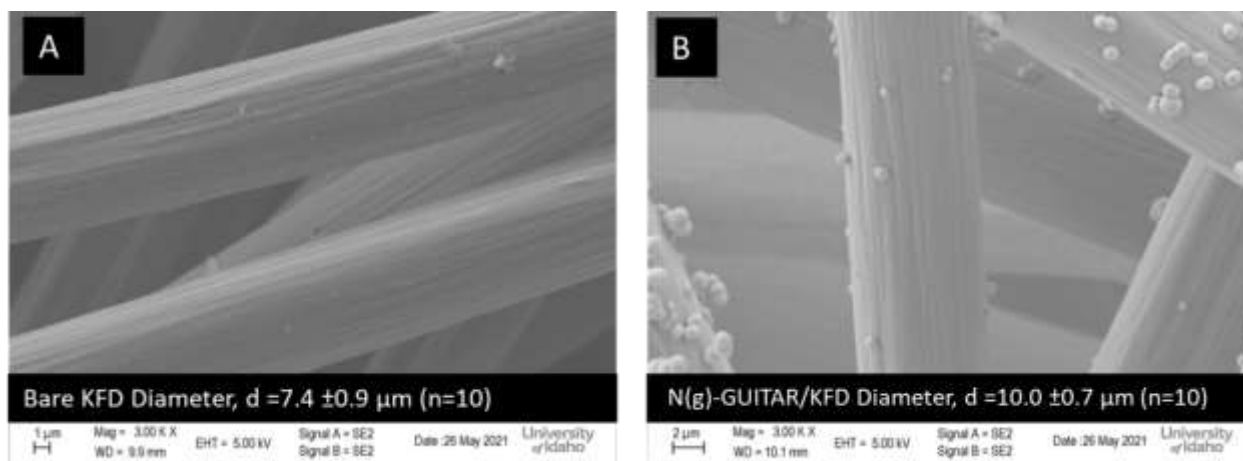

Figure 3. *A) Scanning electron micrographs (SEM) micrographs of as obtained KFD felt. B) N(g)-GUITAR coated KFD. The average diameter KFD fiber is 7.4± 0.9 μm (n = 10) and for N(g)-GUITAR/KFD is 10.0 ± 0.7 μm (n = 10). These measurements were estimated with ImageJ software*

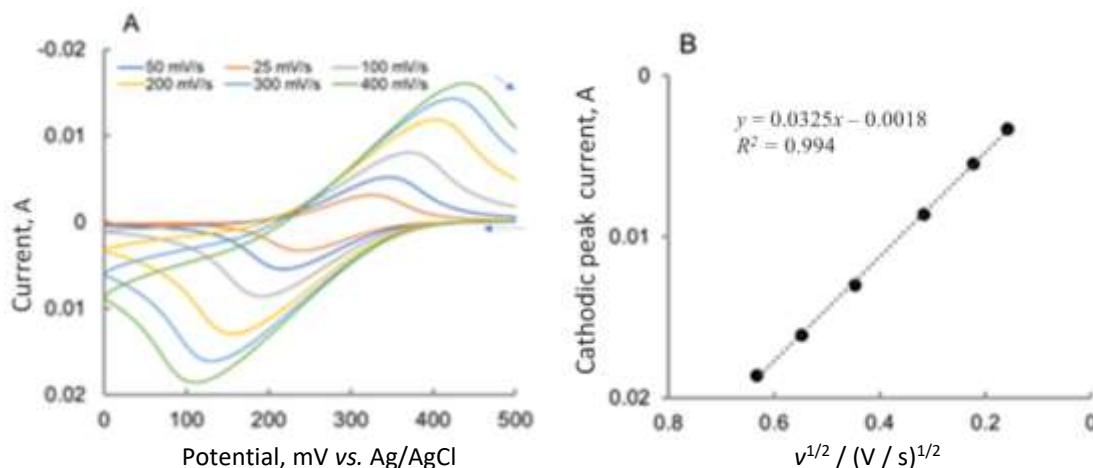**Figure 4.** *A) Cyclic voltammograms (CV) obtained at various scan rates of 1 mM Fe(CN)$_6^{3-/4-}$ in 1 M KCl. (B) Cathodic peak current (i$_p$) vs. square root of scan rate for the estimation of the electrochemically active surface area (ECSA) from the Randles-Ševčik equation. The best fit line indicates semi-infinite linear diffusion*

Cyclic voltammetric studies

The electrocatalysts were examined for ORR activity by CV in 0.05 M Na$_2$SO$_4$ at 50 mV s^{-1} under O$_2$ and Ar purged conditions, as shown in Figure 5. Under O$_2$ purge, GUITAR/KFD exhibits two peak potentials (E_p's) of -0.65 and -1.10 V. This electrolyte is a wastewater surrogate often used in lite-rature [28,29]. Based on literature, this is an indication of the 2e$^-$ process ORR through equation (1)

and the subsequent consumption of H_2O_2 through the reaction of Equation 4 [30-32]. In the case of N(g)-GUITAR/KFD, there is only a single E_p at -0.77 V, which qualitatively indicates $2e^-$ transfer giving H_2O_2 in the ORR of Equation (1), without consumption of H_2O_2 through Equation 4, This will be examined in detail below. Also notable is the relatively large peak current (i_p) of 7.0 mA cm^{-2}at 50 mV s^{-1}, which is the highest reported in the literature (0.7- 4.5 mA cm^{-2}) [30-33]. The i_p based on ECSA is 0.12 mA cm^{-2}. The CVs for both electrode materials under Ar purge indicate an overpotential of about 1 V for the HER (Equation 3).
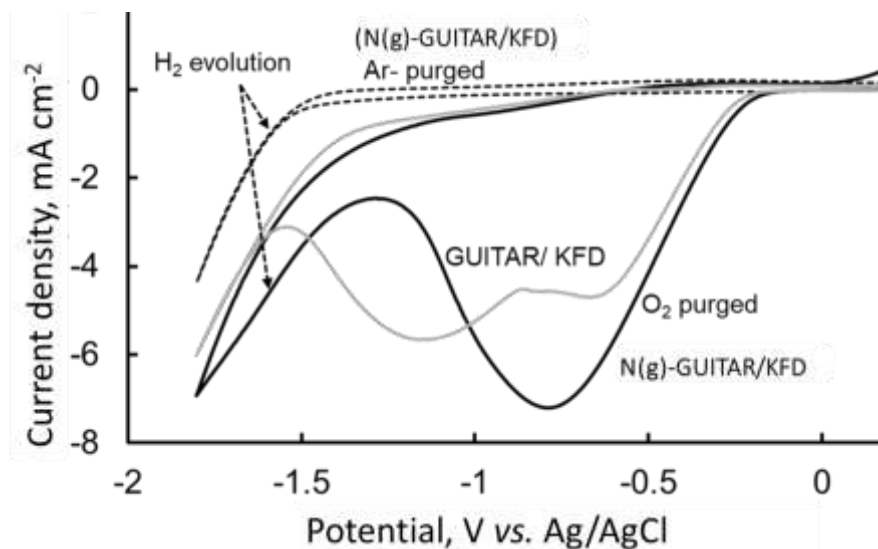

Figure 5. *Cyclic voltammograms at 50 mV/s in 0.05 M Na_2SO_4 under O_2 and Ar saturated conditions for N(g)-GUITAR/KFD and KFD electrodes. The peak potentials (E_p) for GUITAR/KFD are -0.65 and -1.10 V and for N(g)-GUITAR is -0.77 V. The hydrogen evolution reaction (HER) for the scans is also indicated*

H_2O_2 production is the major pathway for the N(g)-GUITAR electrocatalyst

The electrocatalyst was evaluated for generation of H_2O_2 by controlled potential electrolysis (CPE) at potentials ranging from -0.35 to -1.50 V *vs.* Ag/AgCl for 30 min in O_2 saturated 0.05 M Na_2SO_4(aq). The saturation is ensured by bubbling O_2 across the electrode surface, which also aids in mass transport. The N(g)-GUITAR cathode ECSA is 260 cm^2, corresponding to a geometric area of 4.4 cm^2. Control electrodes of the same geometric areas include GUITAR/KFD (ESCA 223 cm^2) and KFD (ECSA 270 cm^2). Selected current-time profiles with the N(g)-GUITAR/KFD cathode are shown in Figure 6A. All chronoamperograms remained at a steady state during the electrolysis for each potential. This is an indication of constant mass transport of O_2 to the electrode and stable electrocatalyst performance. Figure 6C shows the time profile for H_2O_2 concentration at the applied potential of -1.50 V for N(g)-GUITAR/KFD. Data was obtained by taking 0.5 ml aliquots every 5 min for H_2O_2 analysis. This system obeys zero-order kinetics with the observed linear increase in H_2O_2 concentration in Figure 6C. These results show the typical behavior in comparison to other electrochemical H_2O_2 generation studies in the literature [34,35]. The performance of the control electrodes, GUITAR/KFD and KFD, are also shown in Figure 6C. As can be observed through the slopes, the N-doped material is a much more efficient electrocatalyst than either of the control electrodes. Figure 6B illustrates the effect of driving potential on the rates of H_2O_2 production ($\mu mol\ cm^{-2}\ h^{-1}$). The N(g)-GUITAR/KFD electrode increased the H_2O_2 generation rate proportionally with driving potential from the range -0.35 to -1.50 V. Both control electrodes decreased in production rate beyond -0.95 V. It is surprising that GUITAR/KFD is much less efficient than bare KFD. This may be from the consumption of H_2O_2

through Reaction 4 and may be observed in the 2nd CV wave at E_p -1.1 V for GUITAR/KFD in Figure 5. Further evidence is presented in the current efficiency studies below.
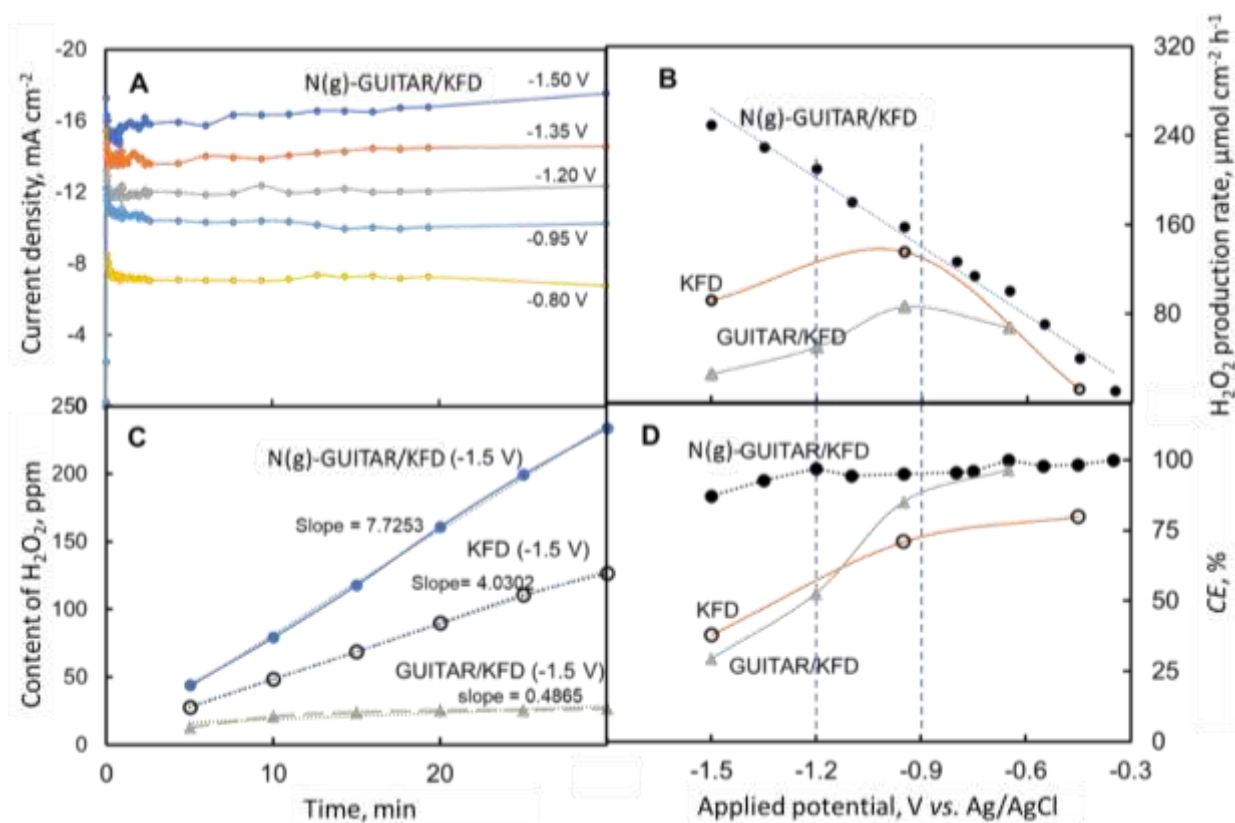

Figure 6. *(A) Current-time curves recorded in O_2 saturated 0.05 M Na_2SO_4 at various constant electrode potentials. (B) Amount of H_2O_2 generated during constant potential analysis and normalized for geometric area. (C) Concentration of measured H_2O_2 with time. (D) Plot of current efficiency for H_2O_2 production at different applied potential*

Under O_2 purge, the controlled potential electrolysis gave pH shifts from pH 7.0 to approximately pH 12. The final pH is expected from the reactions of Equations 1, 2 and 4. A Pourbaix diagram in Figure 7 illustrates that this shift in pH does not affect the spontaneity of reactions electrode potentials from -0.35 V to -1.50 V *vs.* Ag/AgCl.

The current efficiency ($CE_{H_2O_2/O_2}$) for H_2O_2 production was examined for each of three electrode systems of this study. This is described in Equation 6 where *n* is a number of electrons transferred in the balanced half-reaction, *F* is Faraday's constant, *V* is a volume of the cell, and *i* is current [36].

$$CE_{H_2O_2/O_2} = \frac{nFVc_{H_2O_2}}{\int_0^t idt} 100 \qquad (6)$$

Figure 6D demonstrates that N(g)-GUITAR/KFD maintains excellent CE $_{H_2O_2/O_2}$ at all potentials. At the highest driving potential of -1.5 V, it has a $CE_{H_2O_2/O_2}$ of 88 %, at -1.2 V it is 95 % (also see Table 2, Column D). The $CE_{H_2O_2/O_2}$ for both KFD and GUITAR/KFD are notably lower, at 38 % and 29 %, respectively at -1.5 V *vs.* Ag/AgCl. This shows that both control electrodes increase H_2O_2 production rates from -0.35 to 0.95 V with noticeable drops at higher driving potentials. This may be from the consumption of H_2O_2 *via* Reaction 4 and the parasitic HER. These issues do not affect N(g)-GUITAR/KFD performance, as the H_2O_2 production rate increases with increasing cathodic potential.
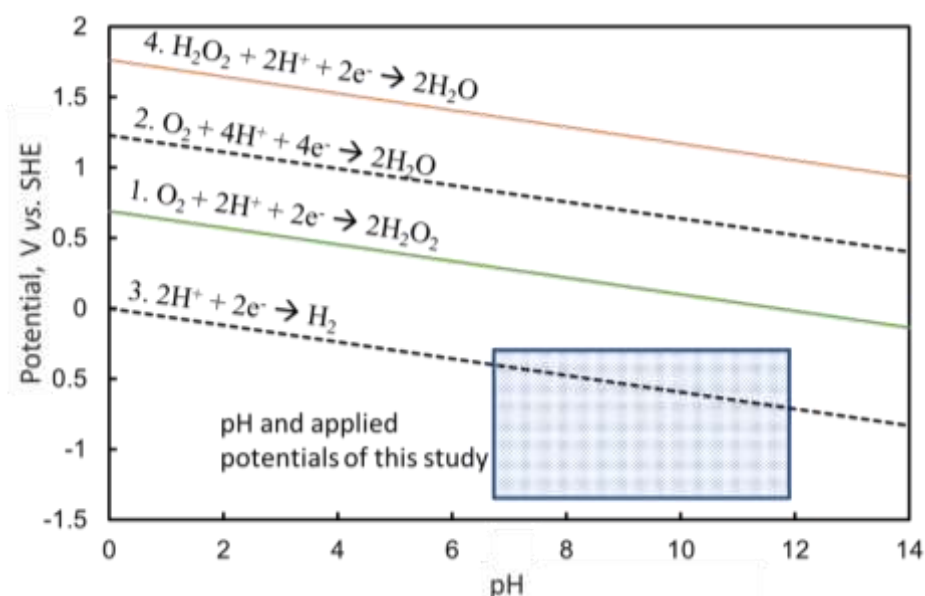
Figure 7. *Pourbaix diagram for the reactions in Equations 1-4. The shaded region are the pH and potential conditions of this study*

Figure 6D demonstrates that N(g)-GUITAR/KFD maintains excellent $CE_{H_2O_2/O_2}$ at all potentials. At the highest driving potential of -1.5 V, it has a $CE_{H_2O_2/O_2}$ of 88 %, at -1.2 V it is 95 % (also see Table 2, Column D). The $CE_{H_2O_2/O_2}$ for both KFD and GUITAR/KFD are notably lower, at 38 and 29 %, respecttively at -1.5 V *vs*. Ag/AgCl. This shows that both control electrodes increase H_2O_2 production rates from -0.35 to 0.95 V with noticeable drops at higher driving potentials. This may be from the consumption of H_2O_2 *via* Reaction 4 and the parasitic HER. These issues do not affect N(g)-GUITAR/KFD performance, as the H_2O_2 production rate increases with increasing cathodic potential.

In general, N(g)-GUITAR operates at a higher *CE* relative to literature electrocatalysts. Figure 8 illustrates the competitiveness of this electrocatalyst at the various applied potentials relative to the literature on non-metal electrocatalysts. Also included are the control surfaces of GUITAR and bare KFD at their maximum *CE* and production rate.
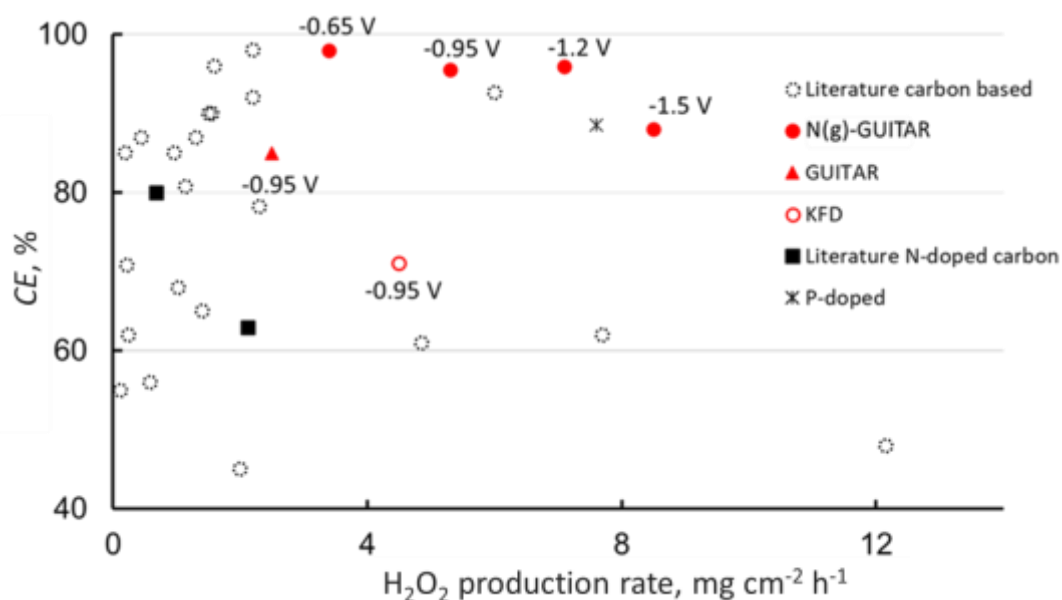

Figure 8. *Plot of H_2O_2 production rate and current efficiency for the N(g)-GUITAR ORR electrocatalyst. The applied potentials are indicated. The highest rates of H_2O_2 production for GUITAR and KFD are included along with literature electrocatalysts [34,35,37-49]*

This N-doped pseudo-graphite electrode operates at 95 to 100 % $CE_{H_2O_2/O_2}$ at potentials ranging from -0.35 to -1.2 V (Figure 6D), while literature electrodes are at 45 to 95 % at similar potentials at lower H_2O_2 production rates [34,35,37-39]. This gives N(g)-GUITAR the ability to effectively operate at higher driving potentials without a loss in *CE*. At the highest potential of this study, -1.50 V *vs.* Ag/AgCl, this electrocatalyst operates at 88 % $CE_{H_2O_2/O_2}$ with a production rate of 250 µmol h^{-1} cm^{-2} (8.5 mg h^{-1} cm^{-2}). This is the highest CE reported for this relatively high rate. Higher production rates have been reported in the literature, but they typically come at the cost of a lower $CE_{H_2O_2/O_2}$ [38]. Considering these performance metrics ($CE_{H_2O_2/O_2}$ and H_2O_2 production rate), N(g)-GUITAR has the best combination of high current efficiency and H_2O_2 production rate [34,35,37,38].

The hydrogen evolution reaction is a minor pathway for the electrocatalyst

The high $CE_{H_2O_2/O_2}$ indicates that the major pathway for the electrocatalyst is through Reaction 1. The extent of the HER as a competing pathway is examined under the conditions for the 2e$^-$ ORR. Previous studies of GUITAR and its variants showed that these materials are kinetically slow for HER. Generally, the overpotential is 1 to 1.5 V and is among the highest of all electrode materials [12,13]. The N(g)-GUITAR/KFD cathode was examined for the HER by chronoamperometry in Ar-purged 0.05 M Na$_2$SO$_4$ at -0.95, -1.20 and -1.50 V *vs.* Ag/AgCl. Figure 9 shows the respective chronoamperograms for this study. In the absence of O$_2$ the charge from those currents is proportional to total H$_2$ production. These charges are summarized in Table 2, Column A. When compared the charge obtained under saturated O$_2$ conditions in Figure 6A and summarized in Table 2 Column B, the HER is a minor component of overall cathodic current ranging from 0.2 % at -0.95 V to 7.8 % at -1.5 V (Table 2 Column C).
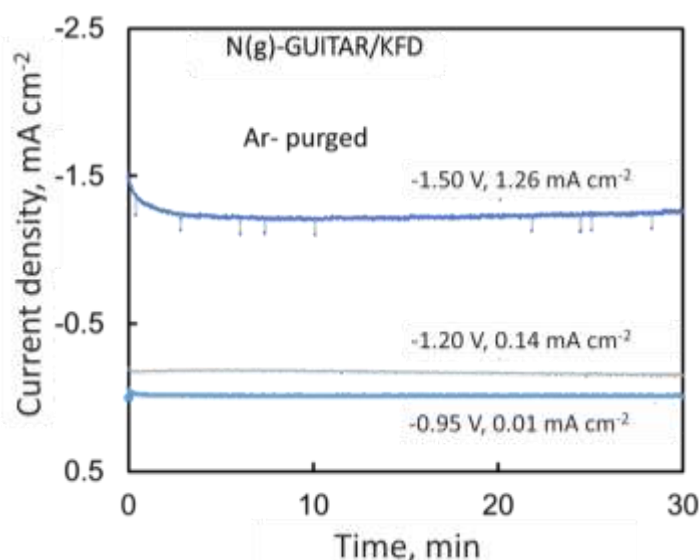

Figure 9. *Chronoamperograms recorded in Ar purged 0.05M Na$_2$SO$_4$. The potentials and steady-state currents for the N(g)-GUITAR/KFD electrodes are described in the diagram*

Assessment of the contribution of the 4e$^-$ ORR pathway to the overall cathodic current: rotating disk electrode studies

The contribution of the 4e$^-$ ORR (Equation 2) to the overall cathodic current was estimated through the measurement of *n*, the number of electrons transferred in the half-reaction. Contributions to ORR through the reaction in Equation 2 occur with *n* > 2. To assess this characteristic, rotating disk electrode (RDE) experiments were conducted. The value, *n* is obtained through the Koutecky-Levich (K-L) relationship in Equation 7. Symbols *J*, *J*$_{k'}$ and *ω* are the current density,

kinetic current density, and angular velocity, respectively. In the K-L equation, B is $0.62nFv^{1/6}$ $c_{O_2}D_{O_2}^{2/3}$, where F is Faraday's constant, v is the kinematic viscosity of the electrolyte (0.01 cm^2 s^{-1}), c_{O_2} is the bulk concentration of oxygen (1.20×10^{-6} mol cm^{-3}) and D_{O_2} is the diffusion coefficient of O_2 in 0.050 M Na_2SO_4 (1.90×10^{-5} cm^2 s^{-1}) [15,36].

$$\frac{1}{J} = \frac{1}{J_k} + \frac{1}{B\omega^{1/2}} \tag{7}$$

For the RDE study, the graphitic nitrogen-rich N(g)-GUITAR electrocatalysts were deposited on Ketjen black particles as described in the experimental and previous studies [15]. In previous investigations, pristine GUITAR had $n = 2.6$ to 2.8 and a variant of an N-doped GUITAR (N´-GUITAR) which had a predominance of pyridinic and pyrrolic moieties, was found to have $n = 3.6$ to 3.7 [15]. The background corrected RDE linear sweep voltammograms (5 mV s^{-1}) from 400 to 2400 rpm are shown in Figure 10A. Between the potential range of -0.7 to -1.5 V *vs.* Ag/AgCl, this electrocatalyst was found to have $n = 1.99$ (see Figure 10B). This, along with CE data of Section 3.3, strongly indicate that this electrocatalyst has a strong preference for Reaction in Equation 1, with Reaction 2 being a negligible pathway.
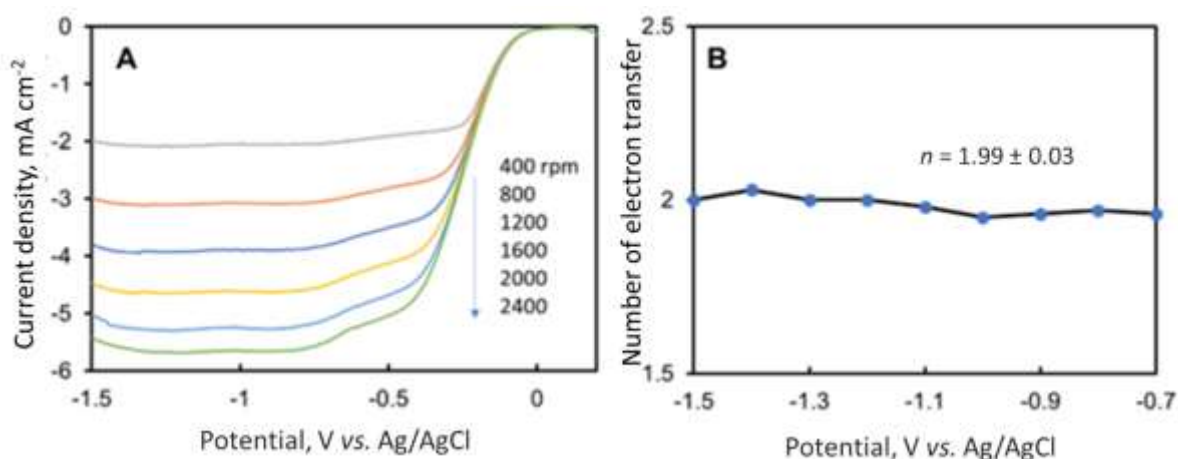

Figure 10. A) Rotating disk electrode (RDE) linear sweep voltammograms recorded at different rotating rates in 0.05 M Na_2SO_4. B) The number of electrons transferred from the Koutecky-Levich equation over the potential range of -0.7 to -1.5 V. The average electrons transferred (n) over the entire potential range with one standard deviation is shown

Other pathways that lead to the loss of H_2O_2

The pathways that lead to the loss of H_2O_2 produced through the 2e$^-$ ORR are the electroreduction of H_2O_2 giving H_2O (Equation 4) and disproportionation through the reaction in Equation 8 [10].

$$2H_2O_2 \rightarrow O_2 + 2H_2O \tag{8}$$

The two reactions cannot be distinguished from one another and therefore are treated together. Equation 2, the 4e- ORR, can also be considered in this analysis. The contribution of these three pathways that lead to the loss of H_2O_2 outlined in Equations 2, 4, and 8 can be inferred from Equation 9, and summarized in Table 2, Column E.

$$\text{Pathways for } H_2O_2 \text{ consumption, \% } = 100 - CE_{H_2} - CE_{H_2O_2/O_2} \tag{9}$$
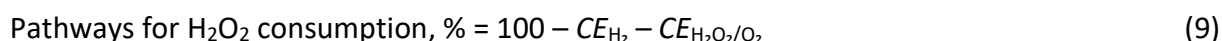
The three values in Column E are not statistically different from each other, it is possible that the disappearance of H_2O_2 is invariant to the applied potentials.

Table 2. *Breakdown of major pathways during oxygen electrolysis in 0.05 M Na$_2$SO$_4$(aq.) for 30 minutes with n = 3. One standard deviation interval is included*

	A	B	C	D	E
Potential, V *vs.* Ag/AgCl	Charge obtained under Ar purge (Fig, 6), C	Charge obtained under O$_2$ purge (Fig. 5A), C	Current efficiency for H$_2$ production *via* Equation 3, %	Current efficiency for H$_2$O$_2$ production *via* Equation 6, %	Pathway for H$_2$O$_2$ degradation pathways (Equations 2, 4 and 7), %
-0.95	0.17 ± 0.04	87.4 ± 5.3	0.2 ± 0.06	96 .0 ± 1.0	3.8 ± 1.0
-1.20	1.42 ± 0.10	100.0 ± 4.5	1.4 ± 0.2	95.0 ± 2.0	3.6 ± 2.0
-1.50	10.5 ± 0.5	134.0 ± 3.6	7.8 ± 0.5	87.8 ± 1.8	4.4 ± 1.8

The N(g)-GUITAR electrocatalyst is stable

The electrocatalyst stability is demonstrated in the sequence of experiments outlined in Figure 11. The electrode was subjected to a constant potential of -1.50 V for five, 30-minute cycles under O$_2$ purged conditions. The H$_2$O$_2$ production rate (Figure 11A) and current efficiencies (Figure 11B) indicate no degradation in catalyst performance.
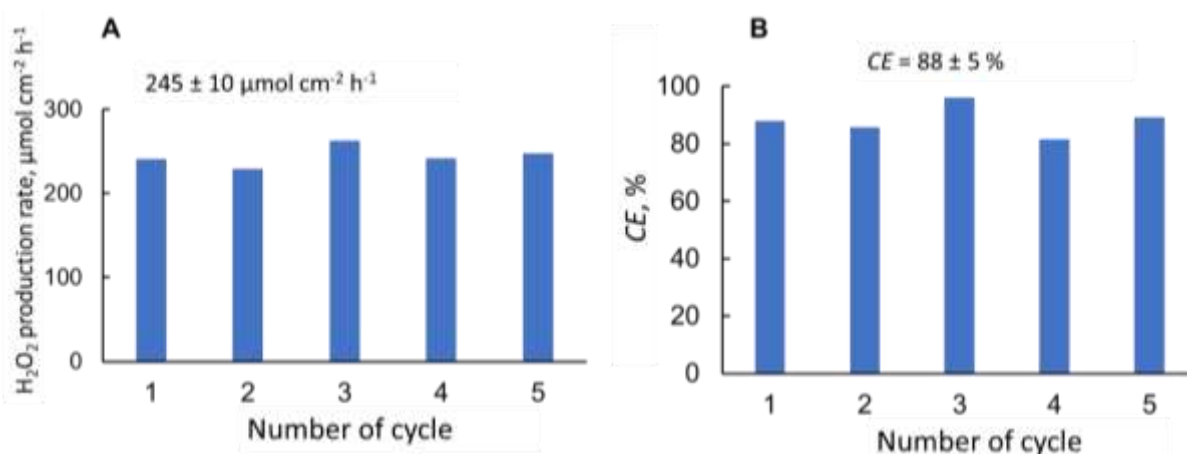
Figure 11. *Stress tests of the N(g)-GUITAR electrode for H$_2$O$_2$ production. Average values and one standard deviation are indicated on each graph. A) Rates of hydrogen peroxide generation at -1.5 V of applied potential in 0.05 M Na$_2$SO$_4$. B) Current efficiencies as calculated using Equation 6*

Summary and conclusions

The ability to selectively dope GUITAR with different nitrogen moieties is unique to this pseudo-graphitic material. Our previous form of nitrogen-doped material, N(py)-GUITAR, contains 0.9 % nitrogen by atomic abundance with the division in those species as 0.0 % graphitic-N, 46.0 % pyridinic, 41.6 % pyrrolic, and 12.4 % N-oxide [15]. That electrocatalyst gave an ORR pathway through a 4e$^-$ mechanism giving H$_2$O (Equation 2). In this study, another form of nitrogen-doped pseudo-graphite, N(g)-GUITAR, has an atomic nitrogen abundance of 9.7 %. Those N species have a division of 72.3 % graphitic N, 23.7 % pyridinic, 0.0 % pyrrolic, and 4.0 % N-oxide [13]. Based on the rotating disk electrode and chronoamperometric studies, N(g)-GUITAR shows a strong preference for the 2e$^-$ route to H$_2$O$_2$ production (Equation 1). This result agrees with the literature and indicates the importance of graphitic N for this pathway [21,23]. While N(g)-GUITAR has a relatively high abundance of pyridinic nitrogen (23.7 %), it was observed that this moiety did not significantly contribute to the 4e$^-$ pathway. This runs contra to literature hypotheses [18]. However, this result must be viewed in the context that GUITAR is a pseudo-graphite with a plethora of structural defects. The preference for the 2e$^-$ ORR pathway along with significant overpotentials for the HER (Equation 3) and H$_2$O$_2$ consumption (Equation 4) gives an electrocatalyst with the highest combination of H$_2$O$_2$ production and current efficiency in literature. The H$_2$O$_2$ production rate from Figure 6C is 106 mg L^{-1} h^{-1} cm^{-2} at -1.50 V and

65 mg L^{-1} h^{-1} cm^{-2} at -0.95 V. This indicates applications in water treatment and wastewater reme-diation, which require 17-68 mg L^{-1} H_2O_2 in conjunction with UV light, and 50-250 mg L^{-1} H_2O_2 for Fenton reaction processes [50,51]. It also can be used directly as a disinfectant which requires 10-100 mg L^{-1} of H_2O_2 [52]. It should be expected that higher H_2O_2 production rates can be obtained with optimized cell and high surface area electrode configurations.

References

[1] R. Ciriminna, L. Albanese, F. Meneguzzo, M. Pagliaro, Hydrogen peroxide: A key chemical for today's sustainable development, *ChemSusChem* **9** (2016) 3374-3381. https://doi.org/10.1002/cssc.201600895

[2] J. M. Campos-Martin, G. Blanco-Brieva, J. L. G. Fierro, Hydrogen peroxide synthesis: An outlook beyond the anthraquinone process, *Angewandte Chemie International Edition* **45** (2006) 6962-6984. https://doi.org/10.1002/anie.200503779

[3] S. Siahrostami, S. J. Villegas, A. H. Bagherzadeh Mostaghimi, S. Back, A. B. Farimani, H. Wang, K. A. Persson, J. Montoya, A review on challenges and successes in atomic-scale design of catalysts for electrochemical synthesis of hydrogen peroxide, *ACS Catalysis* **10** (2020) 7495-7511. https://doi.org/10.1021/acscatal.0c01641

[4] K. Gopal, S. S. Tripathy, J. L. Bersillon, S. P. Dubey, Chlorination byproducts, their toxicodynamics and removal from drinking water, *Journal of Hazardous Materials* **140** (2007) 1-6. https://doi.org/10.1016/j.jhazmat.2006.10.063

[5] S. Yang, A. Verdaguer-Casadevall, L. Arnarson, L. Silvioli, V. Čolić, R. Frydendal, J. Rossmeisl, I. Chorkendorff, I. E. L. Stephens, Toward the decentralized electrochemical production of H_2O_2: A focus on the catalysis, *ACS Catalysis* **8** (2018) 4064-4081. https://doi.org/10.1021/acscatal.8b00217

[6] E. Jung, H. Shin, W. Hooch Antink, Y.-E. Sung, T. Hyeon, Recent advances in electrochemical oxygen reduction to H_2O_2: Catalyst and cell design, *ACS Energy Letters* **5** (2020) 1881-1892. https://doi.org/10.1021/acsenergylett.0c00812

[7] J. Gao, B. Liu, Progress of electrochemical hydrogen peroxide synthesis over single atom catalysts, *ACS Materials Letters* **2** (2020) 1008-1024. https://doi.org/10.1021/acsmaterialslett.0c00189

[8] C. Badellino, C. A. Rodrigues, R. Bertazzoli, Oxidation of pesticides by in situ electrogenerated hydrogen peroxide: Study for the degradation of 2,4-dichlorophenoxyacetic acid, *Journal of Hazardous Materials* **137** (2006) 856-864. https://doi.org/10.1016/j.jhazmat.2006.03.035

[9] W. Zhou, X. Meng, J. Gao, A. N. Alshawabkeh, Hydrogen peroxide generation from O_2 electroreduction for environmental remediation: A state-of-the-art review, *Chemosphere* **225** (2019) 588-607. https://doi.org/10.1016/j.chemosphere.2019.03.042

[10] G. Xia, Y. Lu, H. Xu, Electrogeneration of hydrogen peroxide for electro-Fenton via oxygen reduction using polyacrylonitrile-based carbon fiber brush cathode, *Electrochimica Acta* **158** (2015) 390-396. https://doi.org/10.1016/j.electacta.2015.01.102

[11] J. Song, S. Cho, Catalytic materials for efficient electrochemical production of hydrogen peroxide, *APL Materials* **8** (2020) 050701. https://doi.org/10.1063/5.0002845

[12] H. Kabir, H. Zhu, J. May, K. Hamal, Y. Kan, T. Williams, E. Echeverria, D.N. McIlroy, D. Estrada, P.H. Davis, T. Pandhi, K. Yocham, K. Higginbotham, A. Clearfield, I.F. Cheng, The sp^2-sp^3 carbon hybridization content of nanocrystalline graphite from pyrolyzed vegetable oil, comparison of electrochemistry and physical properties with other carbon forms and allotropes, *Carbon N Y.* **144** (2019) 831-840. https://doi.org/10.1016/j.carbon.2018.12.058

[13] K. Hamal, J. May, H. Zhu, F. Dalbec, E. Echeverria, D. N. McIlroy, E. Aston, I. F. Cheng, Electrochemical aspects of a nitrogen-doped pseudo-graphitic carbon material: Resistance

to electrode fouling by air-aging and dopamine electro-oxidation, *C-Journal of Carbon Research (Basel)* **6** (2020) 68. https://doi.org/10.3390/c6040068

[14] I.O. Gyan, P. M. Wojcik, D. E. Aston, D. N. McIlroy, I. F. Cheng, A study of the electrochemical properties of a new graphitic material: GUITAR, *ChemElectroChem* **2** (2015) 700-706. https://doi.org/10.1002/celc.201402433

[15] K. Hamal, J. May, D. Koirala, H. Zhu, H. Kabir, E. Echeverria, D. N. McIlroy, N. Nicholas, I. F. Cheng, Highly stable, low-cost metal-free oxygen reduction reaction electrocatalyst based on nitrogen-doped pseudo-graphite, *Energy & Fuels* **35** (2021) 10146-10155. https://doi.org/10.1021/acs.energyfuels.1c00658

[16] H. Kabir, I. Gyan, J. Foutch, H. Zhu, I. Cheng, Application of GUITAR on the negative electrode of the vanadium redox flow battery: Improved $V^{3+/2+}$ heterogeneous electron transfer with reduced hydrogen gassing, *C-Journal of Carbon Research (Basel)* **2** (2016) 13. https://doi.org/10.3390/c2020013

[17] D. Guo, R. Shibuya, C. Akiba, S. Saji, T. Kondo, J. Nakamura, Active sites of nitrogen-doped carbon materials for oxygen reduction reaction clarified using model catalysts, *Science* **351** (2016) 361-365. https://doi.org/10.1126/science.aad0832

[18] K. Gong, F. Du, Z. Xia, M. Durstock, L. Dai, Nitrogen-doped carbon nanotube arrays with high electrocatalytic activity for oxygen reduction, *Science* **323** (2009) 760-764. https://doi.org/10.1126/science.1168049

[19] R. Ma, G. Lin, Y. Zhou, Q. Liu, T. Zhang, G. Shan, M. Yang, J. Wang, A review of oxygen reduction mechanisms for metal-free carbon-based electrocatalysts, *NPJ Computational Materials* **5** (2019) 78. https://doi.org/10.1038/s41524-019-0210-3

[20] N. P. Subramanian, X. Li, V. Nallathambi, S. P. Kumaraguru, H. Colon-Mercado, G. Wu, J.-W. Lee, B.N. Popov, Nitrogen-modified carbon-based catalysts for oxygen reduction reaction in polymer electrolyte membrane fuel cells, *Journal of Power Sources* **188** (2009) 38-44. https://doi.org/10.1016/j.jpowsour.2008.11.087

[21] J. Zhang, G. Zhang, S. Jin, Y. Zhou, Q. Ji, H. Lan, H. Liu, J. Qu, Graphitic N in nitrogen-doped carbon promotes hydrogen peroxide synthesis from electrocatalytic oxygen reduction, *Carbon N Y.* **163** (2020) 154-161. https://doi.org/10.1016/j.carbon.2020.02.084

[22] L. Lai, J. R. Potts, D. Zhan, L. Wang, C. K. Poh, C. Tang, H. Gong, Z. Shen, J. Lin, R. S. Ruoff, Exploration of the active center structure of nitrogen-doped graphene-based catalysts for oxygen reduction reaction, *Energy & Environmental Science* **5** (2012) 7936-7942. https://doi.org/10.1039/c2ee21802j

[23] E. Contreras, D. Dominguez, H. Tiznado, J. Guerrero-Sanchez, N. Takeuchi, G. Alonso-Nunez, O. E. Contreras, M. T. Oropeza-Guzmán, J. M. Romo-Herrera, N-doped carbon nanotubes enriched with graphitic nitrogen in a buckypaper configuration as efficient 3D electrodes for oxygen reduction to H_2O_2, *Nanoscale* **11** (2019) 2829-2839. https://doi.org/10.1039/C8NR08384C

[24] R. E. G. Smith, T. J. Davies, N. de B. Baynes, R. J. Nichols, The electrochemical characterisation of graphite felts, *Journal of Electroanalytical Chemistry* **747** (2015) 29-38. https://doi.org/10.1016/j.jelechem.2015.03.029

[25] D. Koirala, N. Yensen, P.B. Allen, Open source all-iron battery 2.0, *HardwareX* **9** (2021) e00171. https://doi.org/10.1016/j.ohx.2020.e00171

[26] R. M. Sellers, Spectrophotometric determination of hydrogen peroxide using potassium titanium(IV) oxalate, *Analyst* **105** (1980) 950. https://doi.org/10.1039/an9800500950

[27] X. Huang, Fabrication and properties of carbon fibers, *Materials* **2** (2009) 2369-2403. https://doi.org/10.3390/ma2042369

[28] M. Panizza, G. Cerisola, Electrochemical generation of H_2O_2 in low ionic strength media on gas diffusion cathode fed with air, *Electrochimica Acta* **54** (2008) 876-878. https://doi.org/10.1016/j.electacta.2008.07.063

[29] A. R. Khataee, M. Safarpour, M. Zarei, S. Aber, Electrochemical generation of H_2O_2 using immobilized carbon nanotubes on graphite electrode fed with air: Investigation of operational parameters, *Journal of Electroanalytical Chemistry* **659** (2011) 63-68. https://doi.org/10.1016/j.jelechem.2011.05.002

[30] G. Panomsuwan, N. Saito, T. Ishizaki, Nitrogen-doped carbon nanoparticle–carbon nanofiber composite as an efficient metal-free cathode catalyst for oxygen reduction reaction, *ACS Applied Materials & Interfaces* **8** (2016) 6962-6971. https://doi.org/10.1021/acsami.5b10493

[31] T. Chen, Z. Cai, Z. Yang, L. Li, X. Sun, T. Huang, A. Yu, H.G. Kia, H. Peng, Nitrogen-doped carbon nanotube composite fiber with a core-sheath structure for novel electrodes, *Advanced Materials* **23** (2011) 4620-4625. https://doi.org/10.1002/adma.201102200

[32] Z.-H. Sheng, L. Shao, J.-J. Chen, W.-J. Bao, F.-B. Wang, X.-H. Xia, Catalyst-free synthesis of nitrogen-doped graphene *via* thermal annealing graphite oxide with melamine and its excellent electrocatalysis, *ACS Nano* **5** (2011) 4350-4358. https://doi.org/10.1021/nn103584t

[33] Z. Chen, S. Chen, S. Siahrostami, P. Chakthranont, C. Hahn, D. Nordlund, S. Dimosthenis, J.K. Nørskov, Z. Bao, T.F. Jaramillo, Development of a reactor with carbon catalysts for modular-scale, low-cost electrochemical generation of H_2O_2, *Reaction Chemistry & Engineering* **2** (2017) 239-245. https://doi.org/10.1039/C6RE00195E

[34] Y. Liu, X. Quan, X. Fan, H. Wang, S. Chen, High-yield electrosynthesis of hydrogen peroxide from oxygen reduction by hierarchically porous carbon, *Angewandte Chemie International Edition* **54** (2015) 6837-6841. https://doi.org/10.1002/anie.201502396

[35] W. Yang, M. Zhou, J. Cai, L. Liang, G. Ren, L. Jiang, Ultrahigh yield of hydrogen peroxide on graphite felt cathode modified with electrochemically exfoliated graphene, *Journal of Materials Chemistry A* **5** (2017) 8070-8080. https://doi.org/10.1039/C7TA01534H

[36] A. Bonakdarpour, D. Esau, H. Cheng, A. Wang, E. Gyenge, D. P. Wilkinson, Preparation and electrochemical studies of metal–carbon composite catalysts for small-scale electrosynthesis of H_2O_2, *Electrochimica Acta* **56** (2011) 9074-9081. https://doi.org/10.1016/j.electacta.2011.06.043

[37] L. Zhou, M. Zhou, C. Zhang, Y. Jiang, Z. Bi, J. Yang, Electro-Fenton degradation of p-nitro-phenol using the anodized graphite felts, *Chemical Engineering Journal* **233** (2013) 185-192. https://doi.org/10.1016/j.cej.2013.08.044

[38] L. Zhou, M. Zhou, Z. Hu, Z. Bi, K. G. Serrano, Chemically modified graphite felt as an efficient cathode in electro-Fenton for p-nitrophenol degradation, *Electrochimica Acta* **140** (2014) 376-383. https://doi.org/10.1016/j.electacta.2014.04.090

[39] Y. Xia, H. Shang, Q. Zhang, Y. Zhou, X. Hu, Electrogeneration of hydrogen peroxide using phosphorus-doped carbon nanotubes gas diffusion electrodes and its application in electro-Fenton, *Journal of Electroanalytical Chemistry* **840** (2019) 400-408. https://doi.org/10.1016/j.jelechem.2019.04.009

[40] X. Yu, M. Zhou, G. Ren, L. Ma, A novel dual gas diffusion electrodes system for efficient hydrogen peroxide generation used in electro-Fenton, *Chemical Engineering Journal* **263** (2015) 92-100. https://doi.org/10.1016/j.cej.2014.11.053

[41] Y. Sheng, S. Song, X. Wang, L. Song, C. Wang, H. Sun, X. Niu, Electrogeneration of hydrogen peroxide on a novel highly effective acetylene black-PTFE cathode with PTFE film, *Electrochimica Acta* **56** (2011) 8651-8656. https://doi.org/10.1016/j.electacta.2011.07.069

[42]   A. da Pozzo, L. di Palma, C. Merli, E. Petrucci, An experimental comparison of a graphite electrode and a gas diffusion electrode for the cathodic production of hydrogen peroxide, *Journal of Applied Electrochemistry* **35** (2005) 413-419. https://doi.org/10.1007/s10800-005-0800-2

[43]   F. Yu, M. Zhou, X. Yu, Cost-effective electro-Fenton using modified graphite felt that dramatically enhanced on H_2O_2 electro-generation without external aeration, *Electrochimica Acta* **163** (2015) 182-189. https://doi.org/10.1016/j.electacta.2015.02.166

[44]   X. Xu, J. Chen, G. Zhang, Y. Song, F. Yang, Homogeneous electro-fenton oxidative degradation of reactive brilliant blue using a graphene doped gas-diffusion cathode, *International Journal of Electrochemical Science* **9** (2014) 569-579. http://www.electrochemsci.org/papers/vol9/90200569.pdf

[45]   W. Zhou, Y. Ding, J. Gao, K. Kou, Y. Wang, X. Meng, S. Wu, Y. Qin, Green electrochemical modification of RVC foam electrode and improved H_2O_2 electrogeneration by applying pulsed current for pollutant removal, *Environmental Science and Pollution Research* **25** (2018) 6015-6025. https://doi.org/10.1007/s11356-017-0810-8

[46]   W. Zhou, L. Rajic, Y. Zhao, J. Gao, Y. Qin, A.N. Alshawabkeh, Rates of H_2O_2 electrogeneration by reduction of anodic O_2 at RVC foam cathodes in batch and flow-through cells, *Electrochimica Acta* **277** (2018) 185-196. https://doi.org/10.1016/j.electacta.2018.04.174

[47]   M. Zarei, D. Salari, A. Niaei, A. Khataee, Peroxi-coagulation degradation of C.I. Basic Yellow 2 based on carbon-PTFE and carbon nanotube-PTFE electrodes as cathode, *Electrochimica Acta* **54** (2009) 6651-6660. https://doi.org/10.1016/j.electacta.2009.06.060

[48]   J. Choi, S.H. Hwang, J. Jang, J. Yoon, High yield hydrogen peroxide production in a solid polymer electrolyte electrolyzer with a carbon fiber coated mesh substrate, *Electrochemistry Communications* **30** (2013) 95-98. https://doi.org/10.1016/j.elecom.2013.02.018

[49]   L. Zhou, Z. Hu, C. Zhang, Z. Bi, T. Jin, M. Zhou, Electrogeneration of hydrogen peroxide for electro-Fenton system by oxygen reduction using chemically modified graphite felt cathode, *Separation and Purification Technology* **111** (2013) 131-136. https://doi.org/10.1016/j.seppur.2013.03.038

[50]   J. C. Crittenden, R. R. Trussell, D. W. Hand, K. J. Howe, G. Tchobanoglous, *MWH's Water Treatment*, John Wiley & Sons, Inc., Hoboken, NJ, USA, 2012. https://doi.org/10.1002/9781118131473

[51]   G. R. Agladze, G. S. Tsurtsumia, B.-I. Jung, J.-S. Kim, G. Gorelishvili, Comparative study of chemical and electrochemical Fenton treatment of organic pollutants in wastewater, *Journal of Applied Electrochemistry* **37** (2007) 985-990. https://doi.org/10.1007/s10800-007-9325-1.

[52]   J. B. A. Arends, S. van Denhouwe, W. Verstraete, N. Boon, K. Rabaey, Enhanced disinfection of wastewater by combining wetland treatment with bioelectrochemical H_2O_2 production, *Bioresource Technology* **155** (2014) 352-358. https://doi.org/10.1016/j.biortech.2013.12.058